ANALYSIS OF THE HEAT-SHIELD EXPERIMENT ON THE PIONEER-VENUS ENTRY PROBES

Roy M. Wakefield* and William C. Pitts*
Ames Research Center, NASA, Moffett Field, CA 94035

Downloaded by NASA AMES RESEARCH CENTER on May 15, 2014 | http://arc.aiaa.org | DOI: 10.2514/6.1980-1494

Abstract

Information obtained during work on the experiment includes flight data on heat-shield performance, data from ground-based tests in support of the experiment, and comparison of analytical and experimental results. The flight results were obtained from instrumentation on the heat shields of the four Pioneer-Venus entry probes which entered the atmosphere of Venus on December 9, 1978. The ground-based tests include experiments in plasma-jet facilities, measurement of the thermal properties of the heat-shield material, and determination of the decomposition kinetics and composition of the heat-shield material. The analysis includes comparisons of experimental results and computations of the material performance based on a theoretical modeling.

Introduction

Four probes of the Pioneer-Venus program entered the atmosphere of Venus in December 1978 and sent a variety of data to experimenters on Earth. The heat shields, which protected the probes from the heating of atmospheric entry, were instrumented to provide data during entry. This instrumentation was the Pioneer-Venus Heat-Shield Experiment,[1,2] managed by the Entry Technology Branch at Ames Research Center. The objectives of the Pioneer-Venus Heat-Shield Experiment were to obtain flight data on ablation material behavior in planetary entry, and to determine if ablation performance analysis is valid by making comparisons with the flight data. This paper describes the experiment, the data, and the analyses performed.

Pioneer Venus Mission

The Pioneer-Venus program[3] placed an orbiter spacecraft and a multiprobe spacecraft in the vicinity of Venus in December 1978. One spacecraft orbited Venus while onboard instruments made measurements of the upper atmosphere, ionosphere, gravitational field, and radiation. The multiprobe spacecraft was a bus with four probes which entered the Venusian atmosphere. Instruments in the probes made measurements to determine cloud composition and the composition, structure, and general configuration of the atmosphere. The Pioneer-Venus program was directed by the Project Pioneer Office at Ames Research Center. Hughes Aircraft Company, El Segundo, CA., was the prime contractor; the subcontractor for the heat-shield systems[4] of the entry probes was the Research and Environmental Systems Division of General Electric Company, Philadelphia, PA.

The multiprobe spacecraft, (Fig. 1), had four probes, three small and one large, attached to a bus for launch (August 8, 1978) and transit to Venus. The large probe was separated from the bus 24 days before entry; the small probes were released 4 days later. Bus maneuvers and spin at small-probe release placed a probe on each of the required trajectories to Venus. However, the trajectory of a specific small probe could not be determined in advance. For this reason, all the small probes were identical and were designed to accommodate entry angles from 20° to 75°. On December 9, 1978, the probes simultaneously entered the Venusian atmosphere at four widely separated locations. During entry, the heat shields of the probes were subjected to both convective and radiative heating. Data were taken by the heat-shield instrumentation and accelerometers through the heating phase of entry. Atmospheric-measuring instrumentation was active from completion of the heating phase until the probes impact on the surface of Venus.

Heat-Shield Experiment

The heat shields of the entry probes were instrumented with the thermocouples of the heat-shield experiment. Details of theprobes and instrumentation are shown in Fig. 2. The probes were 45° cones with spherical tips; the heat shields were of a carbon-phenolic material described later. Each probe had two thermocouple installations. On the large probe, the forward thermocouple was located at the stagnation point; the aft thermocouple was located at $S/R = 2.2$. On each small probe, the forward thermocouple was slightly off the stagnation point, at $S/R = 0.3$; the aft thermocouple is located at $S/R = 2.2$. The distances from the heated surface of the heat shield to the thermocouple (nominally 0.41 cm at the forward thermocouples and 0.30 cm at the aft thermocouples) were selected so that the thermocouples would respond to the various entry heating phenomena. Each thermocouple installation was comprised of a thermocouple plug, which was inserted in a flat-bottomed hole drilled from the unheated side of the heat shield. (Heat-shield thickness at the thermocouple installations was approximately 1 cm at the forward thermocouples and approximately 0.75 cm at the aft thermocouple.) The thermocouple plug was a cylindrical piece of heat-shield material slotted for emplacement of a 0.062-cm-diameter ceramic insulator with two holes for the thermocouple wires. At the end of the insulator, the wires were bent so that the 0.002-cm-thick thermocouple junction was flat at the center of the plug. The Type K thermocouples (chromel-alumel) had a maximum service temperature of approximately 1530 K. The output of the thermocouple was digitized by the onboard data-processing system for transmission by telemetry. Time intervals between data points were 0.5 sec for the large probe and 1 sec for the small probes. Each transmitted data

*Research Scientist.

This paper is declared a work of the U.S. Government and therefore is in the public domain.

Downloaded by NASA AMES RESEARCH CENTER on May 15, 2014 | http://arc.aiaa.org | DOI: 10.2514/6.1980-1494

point was processed in an eight-step digitizing cycle; each step in the cycle was 1/64 the interval between data points. Resistance thermometers were used to monitor the temperature of the cold junctions of the thermocouples; these reference temperatures were also transmitted as data.

Flight Data

The four probes all had 11.54-km/sec velocity at 200-km altitude, but different flight pathangles (γ), which resulted in different entry conditions for each probe. The day probe, with $\gamma = -25.4^{o}$, was subjected to entry heating for approximately 7 sec, and the resulting response of the thermocouples is shown in Fig. 3(a). The large probe, with $\gamma = -32.4^{o}$, was subjected to approximately 5 sec of heating[5], and the resulting thermocouple response is shown in Fig. 3(b). The night probe, with $\gamma = -41.5^{o}$, received heating for approximately 4 sec[5], and the response of the thermocouples is shown in Fig. 3(c). The north probe, with $\gamma = -68.7^{o}$, was subjected to heating for approximately 3 sec, and the response of the thermocouples is shown in Fig. 3(d). (Flight data are listed in Table 1.) For all four probes, there is a well-defined increase in thermocouple temperature. In the results shown in Fig. 3, the shapes of the temperature-time histories for the forward thermocouples (stagnation point and S/R = 0.3) differ for the four probes. In contrast, the temperature-time histories for the aft thermocouples (S/R = 2.2) are very similar. Each respective temperature-time history is the coupled effect of the convective and radiative heating at the thermocouple location, the boundary-layer phenomena that affect the fraction of the entry heating reaching the heat-shield surface, the heat shield material response, and the depth of the thermocouples below the surface of the heat shield. These effects will be discussed further in the analysis.

Entry Heating Conditions

The entry heating conditions have been determined (from other experiments and analysis) for the day probe and the north probe. The values of velocity, atmospheric density, and pressure determined in the Atmosphere Structure Experiment[6] were used by Sutton and Zoby of Langley Research Center to compute heating fluxes with their approximate methods[7,8]. (Results for the large probe and the night probe from the Atmosphere Structure Experiment were not available in time for computation of the heating conditions for this paper.) Heating conditions at the forward thermocouples are shown in Fig. 4(a). Fluxes illustrated are the laminar convective heating and radiative heating. The significant differences in the conditions for the two trajectories are that the north probe had the higher peak convec.ive and radiative fluxes and also the higher ratio of the peak values of radiative to convective fluxes. Heating conditions at the aft thermocouples are shown in Fig. 4b. The turbulent flux at the rear thermocouples is higher than the (laminar) convective flux at the forward thermocouple on each probe, and the radiative flux at the aft thermocouples is relatively low. In the present paper, analytical comparisons will be made only with results from the north probe and day probe.

Analytical Method

In the analysis of the Pioneer Venus data, the temperature of a thermocouple imbedded in the ablating heat-shield material was computed with the Charring Material Ablation (CMA) computer program.[9] This program can compute the heat-shield temperature at arbitrary internal locations (as well as other aspects of material behavior) by treating the interacting phenomena of heat-shield ablation. The CMA program output was used as input to a program that simulates the digitizing process on the entry probes.

The CMA computer program and similar programs are widely used at the present time to calculate ablation material behavior.[4] In the analysis, the principal assumptions are: (1) the ablation gases and the boundary layer gases are in chemical equilibrium, (2) the diffusion coefficients of all gases are equal, and (3) the Prandtl and Lewis numbers are unity. Validation of the CMA program for combined convective and radiative heating of graphite has been performed for stagnation point conditions.[10] The inputs for the heat shield that are shield that are needed for the computation are the thermal properties of the ablation material, constants for any rate-limited ablation processes, material thickness, thermocouple depths, and backup material details. For each entry, time variations are specified for the convective flux, radiative flux, surface pressure, and free-stream enthalpy. The transient ablation computations treat the imposed fluxes to determine ablatio n rates, temperature distribution in the ablation material, surface reradiation, and reduction of the convective heating by the ablation products entering the boundary layer. Outputs of the program are the time histories of the surface and internal temperatures and the ablation and degradation rates.

Carbon-Phenolic Heat-Shield Material

Carbon-phenolic material consists of layers of carbon fabric bonded together with phenolic resin. The phenolic resin, when heated, undergoes pyrolysis and is converted to gas and residual carbon. When carbon-phenolic ablates, a graphitic char is formed from the residual carbon and the carbon in the carbon fabric, and a discrete pyrolysis zone is established between the char and the unablated material. Sublimation of the char to release carbon gas may occur and char, pyrolysis gases, and boundary-layer gases may react and result in material loss and surface recession. Loss of surface material in solid particles has been reported for varied materials[11] and may also occur for carbon-phenolic char in char in some entry situations. During entry heating, the exposed char surface ranges from a temperature of 1500 to 3800 K; the pyrolysis zone is 400 to 1200 K. (The

Downloaded by NASA AMES RESEARCH CENTER on May 15, 2014 | http://arc.aiaa.org | DOI: 10.2514/6.1980-1494

thermocouples of the heat-shield experiment were placed at distances from the heated surface to be in the pyrolysis zone during entry heating.) Carbon-phenolic accommodates the heating of atmospheric entry by radiating energy from the surface of the char layer, by convective blockage action of the pyrolysis gases entering the boundary layer, and by endothermic sublimation and pyrolysis reactions. However, char loss in particles is a form of mass loss without significant energy absorption.

Validation of Analytical Method

Tests were performed on the carbon-phenolic ablation material to obtain the property data required for the CMA computations. Material used in the tests was certified by the manufacturer to meet the same specifications as the material used in the heat shields of the probes. Heat of formation of the virgin material was obtained from bomb calorimetry, and constants for an Arrhenius-type model of the pyrolysis reaction were determined from thermal gravimetric analysis experiments.* In addition, the composition and density of the unablated material and char were measured by chemical analysis and used to determine the composition of the pyrolysis gas. (Information on phenolic-carbon is given in Table 2.) The thermal conductivity and specific heat of the virgin carbon-phenolic material were measured from 250 to 480 K and of the char from 250 to 3000 K.[12] The thermal conductivity of carbon phenolic, both the experiment and the variation used in the analysis, is illustrated in Fig. 5(a). Measurements were made on virgin plastic specimens at temperatures below the onset of pyrolysis. For the data on char, carbon-phenolic was fully pyrolyzed in a furnace at 1920 K. Thermal conductivity measurements were then performed on the char specimens to the maximum temperature attainable in the test apparatus. No thermal conductivity measurements were made in the temperature range of the pyrolysis of carbon-phenolic. Instead, measurements on the virgin plastic were extrapolated to 722 K, which is high enough for rapid pyrolysis of phenolic-carbon, and is a reasonable intersection temperature for a nominal low-temperature extrapolation of the fairing of the thermal conductivity data for the char. The same procedure applied to the specific heat data resulted in the enthalpy of carbon-phenolic shown in Fig. 5(b). This combination of virgin plastic and char properties results in thermal properties that are "virgin-plastic-like" at low temperatures and "charlike" at high temperatures. These properties are considered appropriate for calculations for carbon-phenolic, initally virgin plastic, during the part of a heat pulse or trajectory with increasing or steady-state temperature. Finally, the surface emissivity and absorbtivity value was evaluated from calculations for radiative heating only. The measured radiative heating rates were used with all other material properties, and the emissivity and absorbtivity were taken as the value which resulted in agreement between the measured and calculated surface temperatures.

*Calorimetry and TGA experiments were performed by Orval Flowers of Ames Research Center.

The carbon-phenolic properties were used in computations performed with the CMA program for comparison with test results obtained in combined convective and radiative heating in experiments in the Ames Entry Heating Simulator[13] and in a radiative heating facility. Comparison of experiment and analysis for tests in the Entry Heating Simulator for a condition with convective heating of 1400 W/cm^2, air-stream enthalpy of 23300 J/g, and surface pressure of 0.22 atm, are shown in Fig. 6(a). The calculated and experimental surface temperatures are within measurement accuracy. The mass loss results differ by a relatively constant increment, but the slope of the calculated and experimental mass-loss results agree. The experimental results are believed to include a significant mass-loss increment which occurred as the test specimens were moved between the edge of the test stream and the stream centerline, and as the specimens cooled after testing. This belief is supported by the measured surface temperature of 1800 K when the test specimen reached the stream centerline (0 sec exposure time). Also, the calculated results have the expected characteristics of a heated material having an initial period of heat soak followed by ablation. Similar comparisons of results for tests at the same stream condition but with radiative heating of 2300 W/cm^2 are shown in Fig. 6(b). As in the previous case, the calculated surface temperature and mass-loss rates are in good agreement, and the mass-loss results differ by a constant amount. Other tests of carbon-phenolic were performed in radiant heating with specimens having thermocouple installations identical to the the flight experiment. For tests at a radiative heating rate of 600 W/cm^2, with a thermocouple 0.25 cm below the material surface, surface temperature and thermocouple temperature are compared with analysis in Fig. 7. The measured and calculated results are in agreement within measurement accuracy. The cases illustrated in Figs. 6 and 7 are representative of comparisons obtained of tests at eight conditions. The only significant difference between the analysis and experiment was the offset displacement of the measured mass loss and the calculated mass loss, and the calculated results are considered more reliable due to arguments cited. On the basis of these results, it was concluded that the analytical modeling of the carbon-phenolic material was adequate for analysis of the Pioneer Venus Heat-Shield Experiment.

Comparisons with Flight Results

The analytical method previously discussed and the entry conditions for the day probe and north probe were utilized to generate analytical results. A comparison with flight data for the day probe is shown in Fig. 8(a) (open symbols are data previously shown; filled symbols are calculations). The analytical results are truncated because the temperatures calculated exceed the melting point for the thermocouples before a subsequent data point would be digitized. Also, the calculations of the thermocouple temperatures at later times in the trajectory were omitted because the thermal properties used in the analytical model are only appropriate for material increasing in temperature. The calculated results

Downloaded by NASA AMES RESEARCH CENTER on May 15, 2014 | http://arc.aiaa.org | DOI: 10.2514/6.1980-1494

have the same curvature and relationship as the flight data, although the temperature rise times are offset by several sec. Calculated temperature rise occurred 2 to 3 sec after the time Sutton and Zoby obtained for the onset of entry heating (Fig. 4(a)). This is consistent with the thermocouple response in the radiative heating tests (Fig. 7). Also, the flight data show the temperature rise not occurring until after the heat shield had been heated for approximately 5 sec. This seems unlikely because the thermocouples responded to heat pulses as short as 3 sec on the other probes. Actually, there is not yet complete agreement on the times the probes passed through 200-km altitude. Therefore, it is assumed that the difference between the temperature rise times of the calculated and flight results is probably a discrepancy in time adjustments. Then, due to the strong similarity of the calculated and flight results for both the forward and rear thermocouples, it is concluded that the analysis and flight results are in agreement.

The comparison of analysis and flight results for the north probe is shown in Fig. 8(b). In this case, the calculations and flight results for the forward thermocouple (S/R = 0.3) differ appreciably, but the results for the aft thermocouple (S/R = 2.2) are similar. Some differences in the rate of temperature calculated and from flight is not considered serious. In either the calculation or flight, the thermocouple temperature was changing throughout the 0.125-sec interval of data digitization. The calculated results for the highest temperature for the aft thermocouple (1126 K) range from 1020 to 1331 K, and the same condition undoubtedly occurred in the flight case.

Differences between the forward thermocouple of the north probe from flight and calculation cannot yet be explained. The flight data from the forward thermocouple on the north probe do not have any features that would make the data suspect--the data from the forward thermocouple on the north probe have the same characteristics of the forward thermocouples on the large probe and night probe. At least, the flight results for the north probe indicate a lower rate of temperature rise than calculated for the forward thermocouple; this implies that the actual mass loss at the forward thermocouple location was less than calculated (up to approximately peak heating, which is all the trajectory to which the present analysis can be applied).

Concluding Remarks

Only tentative conclusions can be made at this time from the comparisons of the analysis of flight results from the day probe and north probe. The analytical results for the forward thermocouple locations are a reasonable result for the day probe and a conservative result for the north probe. For the aft thermocouple location, analytical results are in agreement with flight data. The calculated temperatures indicate location of the pyrolysis zone of the ablation material, so any conclusions also apply to the mass loss from the ablation material. Therefore, the preliminary conclusion is that the analysis is either a reasonable or a conservative indication of the ablation mass loss during entry into the atmosphere of Venus. This conclusion must be qualified to the period before the peak surface temperature due to the limitations in the thermal properties used in the analysis.

The results for the forward thermocouple of the north probe are intriguing, especially in view of the similarity of the data for the night probe and large probe and the contrast to the day probe. The entry conditions of the north probe had proportionally more radiative heating than the forward thermocouple location of the day probe. The differences between the calculated and flight results is in the direction that would result from boundary-layer blockage of the radiative heating. This question may be resolved by further analysis.

There are several areas of future work on the results from the Pioneer-Venus Heat-Shield Experiment. The flight results from the night probe and large probe will be analyzed when the entry heating conditions are available. There is also the possibility that additional calculations of the entry conditions will be performed to consider the effects of the ablation gasses on the radiative heating.

In Ref. 1, there was a discussion of investigating boundary layer transition and "particulate" char mass loss in the Heat Shield Experiment. Neither area has been specifically treated in this paper. The boundary layer at the aft thermocouple locations was assumed fully turbulent for the entire trajectory. In view of the apparent agreement of the analysis and flight results, additional analysis at this time was not deemed necessary. Also, analysis was not performed for the available postflight trajectories for particulate mass loss because previous analysis of particluate mass loss has shown that the effect would be an increase in the calculated thermocouple temperature. In the only set of flight results that differed significantly from the analysis, the discrepancy would have been increased by including particulate mass loss in the analysis.

Downloaded by NASA AMES RESEARCH CENTER on May 15, 2014 | http://arc.aiaa.org | DOI: 10.2514/6.1980-1494

References

[1]Wakefield, R. M. and Pitts, W. C., "A Description of the Heat-Shield Experiment on the Pioneer-Venus Entry Probes," AIAA Paper 78-917, Palo Alto, CA., 1978.

[2]Pitts, W. C. and Wakefield, R. M., "Performance of Entry Heat Shields on Pioneer-Venus Probes," to be published in Journal of Geophysical Research.

[3]Dorfman, Steven D., "The Pioneer Venus Spacecraft Program," Journal of Spacecraft, Vol. 14, Nov. 1977, pp. 683-689.

[4]Brewer, R. A., "Selection of a Heat Protection System for Venusian Entry," AIAA Paper 75-731, Denver, CO., 1975.

[5]Moss, J. N., Zoby, E. V., and Sutton, K., "A Study of the Aerothermal Environment for the Pioneer Venus Multiprobe Mission," AIAA Paper 77-766, Albuquerque, NM., 1977.

[6]Seiff, A., et al., "Measurements of Thermal Structure and Thermal Contrasts in the Atmosphere of Venus, and Related Dynamical Observations--Results from the Four Pioneer Venus Probes," to be published in the Journal of Geophysical Research.

[7]Zoby, E. V., Moss, J. N., and Sutton, K., "Approximate Convective Heating Equations for Hypersonic Flows," AIAA Paper 79-1078, Orlando, FL., 1979.

[8]Falanga, R. A. and Olstad, W. B., "An Approximate Inviscid Radiating Flow-Field Analysis for Sphere-Cone Venusian Entry Vehicles," AIAA Paper 74-758, Boston, MA., 1974.

[9]Kendall, R. M., Rindal, R. A., and Bartlett, E. P., "Thermocouple Ablation," AIAA Paper 65-642, Monterey, CA., 1965.

[10]Wakefield, R. M. and Peterson, D. L., "Graphite Ablation in Combined Convective and Radiative Heating," Journal of Spacecraft and Rockets, Vol. 10, Feb. 1973, pp. 149-154.

[11]Lundell, J. H. and Dickey, R. R., "The Ablation of Graphitic Materials in the Sublimation Regime," AIAA Paper 72-298, San Antonio, TX., 1972.

[12]"Thermal Property Measurements on a Chopped Molded Carbon Phenolic Material," Rept. SoRI-EAS-77-246-3694-I-F, Southern Research Institute, Birmingham, AL., April 29, 1977.

[13]Peterson, D. L., Gowen, F. E., and Richardson, C., "Design "Design and Performance of a Combined Convective and Radiative Heating Facility," AIAA Paper 71-255, San Antonio, TX., 1971.

Table 1 Heat-shield temperature in Venus entry.

Day probe

Forward thermocouple		Aft thermocouple	
*Time sec	Temperature K	*Time sec	Temperature K
17.0	317.	16.8	290.
18.0	317.	17.8	290.
19.0	323.	18.8	296.
		19.8	296.
21.0	323.	20.8	307.
22.0	328.	21.8	312.
23.0	333.	22.8	323.
24.0	344.	23.8	345.
25.0	387.	24.8	399.
26.0	545.	25.8	577.
27.0	740.	26.8	1467.
28.0	1214.	27.8	1371.
29.0	1355.	28.8	1284.
30.0	1322.	29.8	1257.
31.0	1273.	30.8	1220.
32.0	1224.	31.8	1114.

Large probe

Forward thermocouple		Aft thermocouple	
*Time sec	Temperature K	*Time sec	Temperature K
14.5	291.	15.5	274.
16.0	291.	16.0	280.
16.5	296.	16.5	280.
17.0	302.	17.0	280.
17.5	302.	17.5	286.
18.0	308.	18.0	286.
18.5	308.	18.5	291.
19.0	313.	19.0	291.
19.5	324.	19.5	297.
20.0	325.	20.0	313.
20.5	352.	20.5	335.
21.0	374.	21.0	374.
21.5	406.	21.5	422.
22.0	433.	22.0	899.
22.5	459.	22.5	1271.
23.0	486.	23.0	1270.
23.5	517.	23.5	1200.
24.0	538.	24.0	1158.
24.5	569.	24.5	1089.
25.0	600.	25.0	1012.
25.5	630.	25.5	950.
26.0	630.	26.0	894.
26.5	625.	26.5	849.
27.0	610.	27.0	813.
27.5	615.	27.5	783.
28.0	620.	28.0	758.
28.5	620.	28.5	737.
29.0	620.	29.0	717.
29.5	620.	29.5	702.
30.0	615.	30.0	687.
30.5	615.	30.5	677.
31.0	615.	31.0	661.

Table 1. Concluded.

Night probe

Forward thermocouple *Time sec	Temperature K	Aft thermocouple *Time sec	Temperature K
16.0	306.		
17.1	312.	17.1	284.
18.1	318.	18.1	284.
19.0	329.	19.1	340.
20.0	356.	20.1	1557.
21.0	469.	21.1	1419.
22.0	538.	22.1	1154.
23.0	600.	23.1	948.
24.0	630.	24.1	828.
25.0	645.	25.1	748.
26.0	650.	25.1	702.
27.0	645.	27.1	667.
28.0	640.	28.1	642.
29.0	630.	29.1	621.
30.0	620.		
31.0	615.		
32.0	605.		

North probe

Forward thermocouple *Time sec	Temperature K	Aft thermocouple *Time sec	Temperature K
8.1	312.	8.2	289.
		9.2	295.
10.1	312.	10.2	312.
11.1	318.	11.2	383.
12.1	323.	12.2	782.
13.1	361.	13.2	1265.
14.1	586.	14.2	1052.
15.1	734.	15.2	868.
16.1	774.	16.2	757.
17.1	759.	17.2	686.
18.1	724.	18.2	640.
19.1	699.	19.2	604.

*Time from 200 km altitude referenced to epoch in Universal Time Coordinated as follows:

Day Probe	18:52:18
Large Probe	18:45:33
Night Probe	18:56:03
North Probe	18:49:40

Table 2. Properties of Carbon-Phenolic Material

	Plastic	Gas	Char
Composition			
Carbon	0.898	0.388	1.0
Hydrogen	0.028	0.178	0
Oxygen	0.069	0.434	0
Density, g/cm^3	1.49		1.24
Heat of formation J/g	-372.	0	0
Emissivity and Absorbtivity	0.70 - 0.75		0.70 - 0.75

Decomposition reaction

$$\frac{d\rho}{d\tau} = \alpha e^{-E/T} \rho_0 (\rho/\rho_0)^n$$

ρ	density
ρ_0	initial density
τ	time, sec
T	temperature, K

ρ_0 g/cm^3	α 1/sec	E K	n –	
0.057	1	3544	1.68	622<T>422
0.188	53340	19680	3.81	T>622

Downloaded by NASA AMES RESEARCH CENTER on May 15, 2014 | http://arc.aiaa.org | DOI: 10.2514/6.1980-1494

Downloaded by NASA AMES RESEARCH CENTER on May 15, 2014 | http://arc.aiaa.org | DOI: 10.2514/6.1980-1494

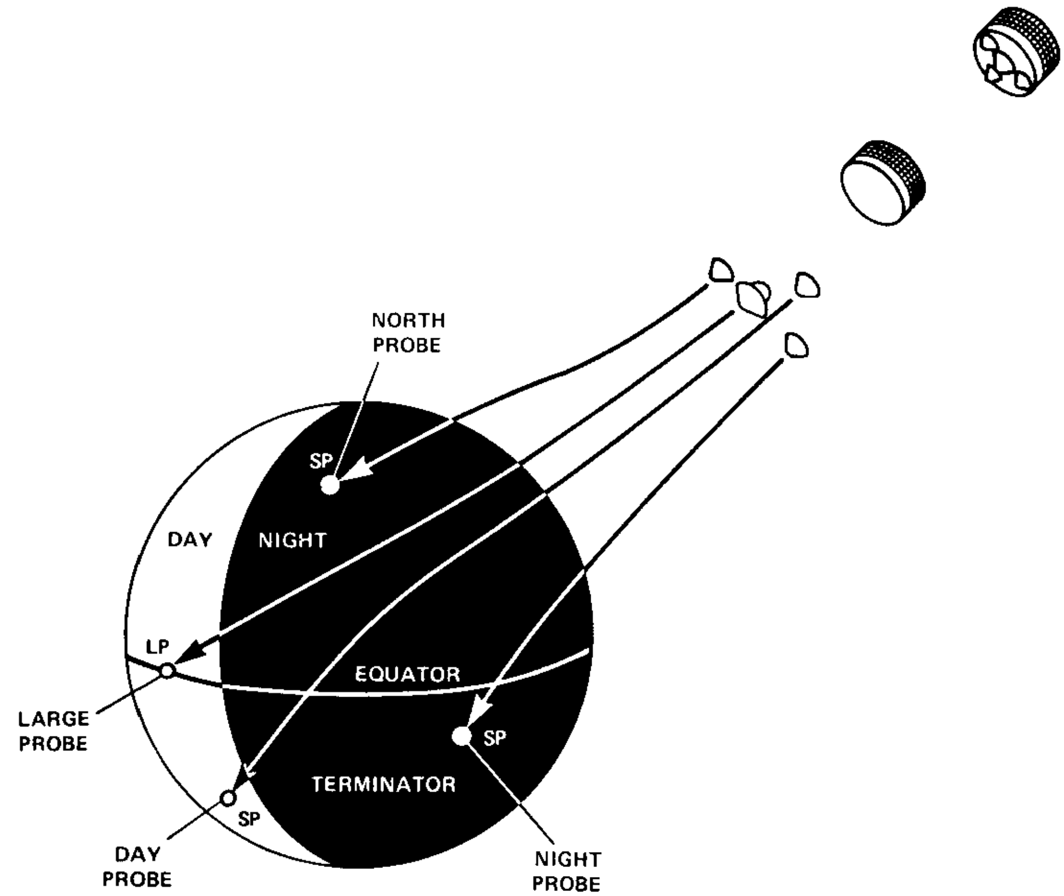

Fig. 1 Pioneer-Vensus multiprobe mission.

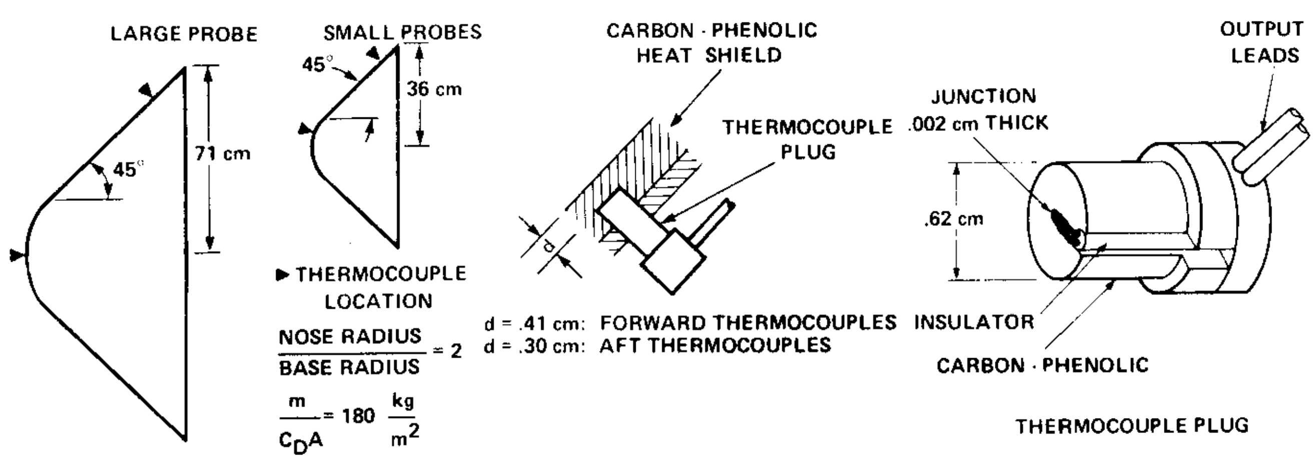

Fig. 2 Details of entry probes and heat-shield thermocouple installations.

Downloaded by NASA AMES RESEARCH CENTER on May 15, 2014 | http://arc.aiaa.org | DOI: 10.2514/6.1980-1494

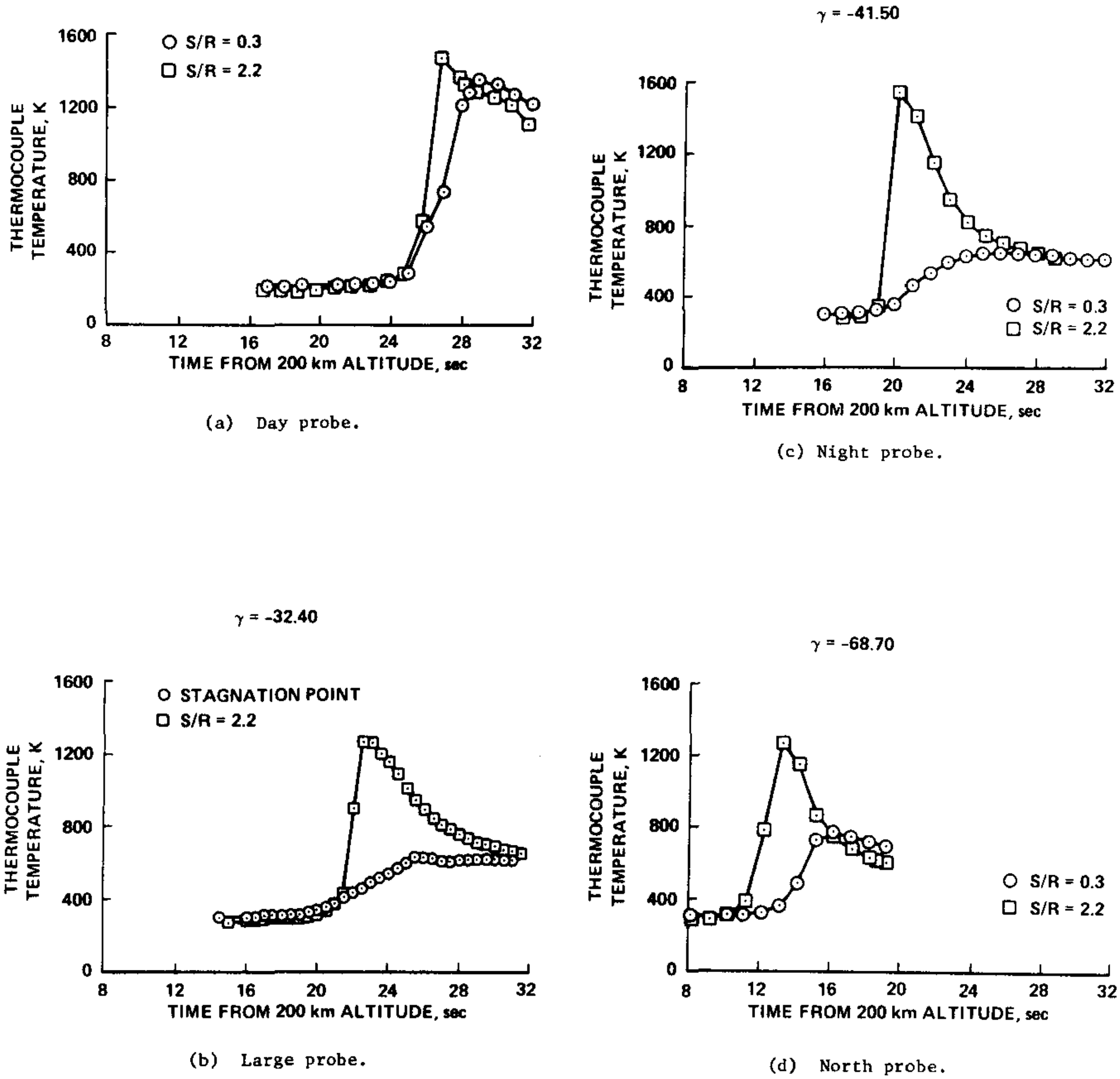

(a) Day probe.

(c) Night probe.

(b) Large probe.

(d) North probe.

Fig. 3 Flight data from heat-shield experiment

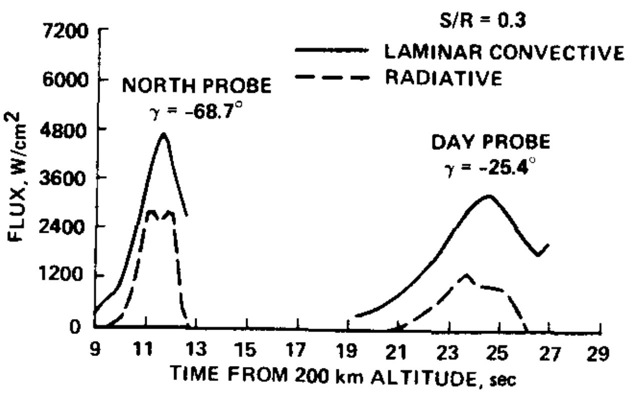

(a) Forward thermocouple locations.

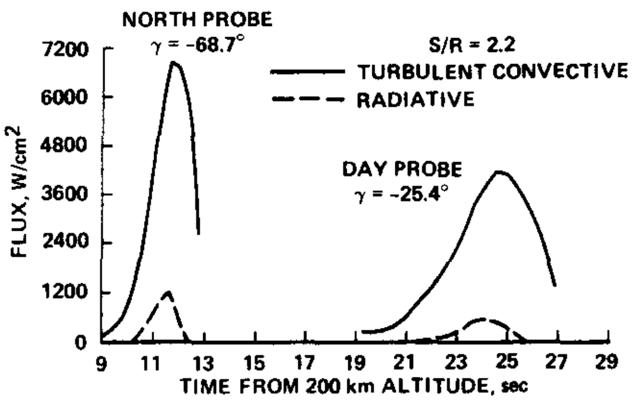

(b) Aft thermocouple locations.

Fig. 4 Entry conditions; trajectories based on flight data.

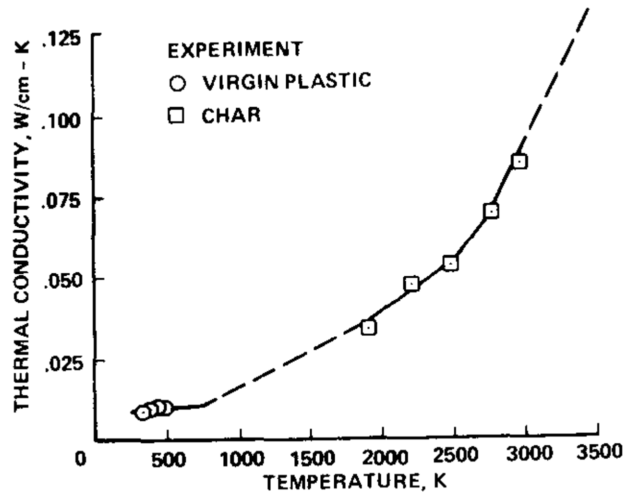

(a) Thermal conductivity.

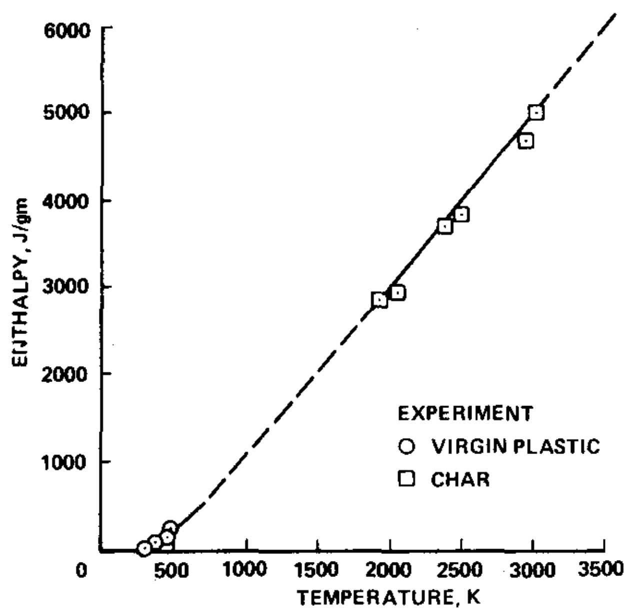

(b) Enthalpy.

Fig. 5 Thermal properties used in analysis of carbon-phenolic heat-shield material.

Downloaded by NASA AMES RESEARCH CENTER on May 15, 2014 | http://arc.aiaa.org | DOI: 10.2514/6.1980-1494

Downloaded by NASA AMES RESEARCH CENTER on May 15, 2014 | http://arc.aiaa.org | DOI: 10.2514/6.1980-1494

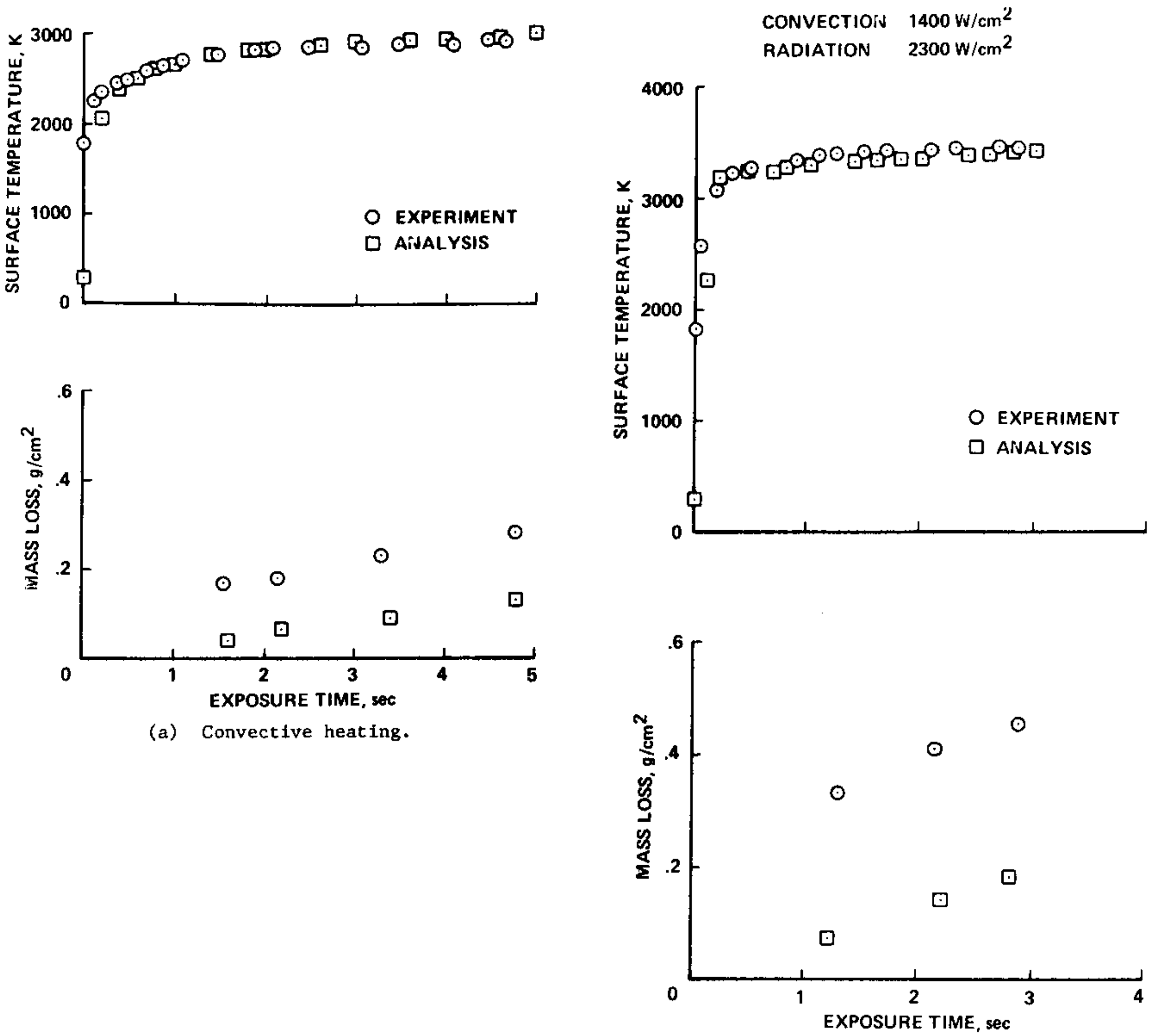

(a) Convective heating.

(b) Combined convective and radiative heating.

Fig. 6 Comparison of experiment and analysis in arc-jet tests.

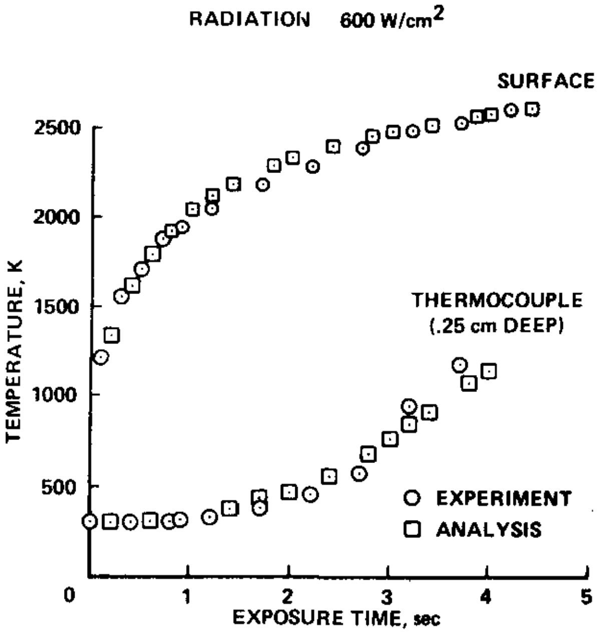

Fig. 7 Comparison of experiment and analysis in radiative heating tests.

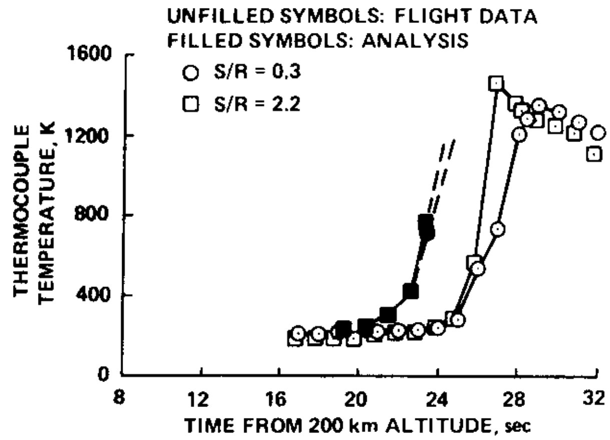

(a) Day probe.

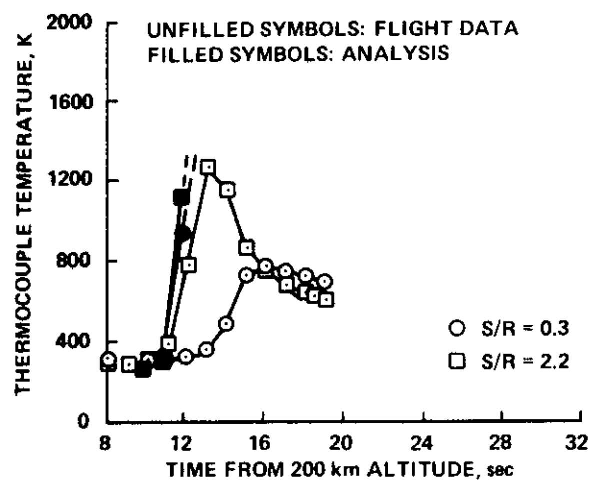

(b) North probe.

Fig. 8 Comparison of experiment and analysis in Venus entry.

Downloaded by NASA AMES RESEARCH CENTER on May 15, 2014 | http://arc.aiaa.org | DOI: 10.2514/6.1980-1494